

Occurrence of a Rare 4<sup>9</sup>·6<sup>6</sup> Structural Topology, Chirality, and Weak Ferromagnetism in the [NH<sub>4</sub>][M<sup>II</sup>(HCOO)<sub>3</sub>] (M = Mn, Co, Ni) FrameworksZheming Wang,<sup>\*,†,‡</sup> Bin Zhang,<sup>†,§</sup> Katsuya Inoue,<sup>||</sup> Hideki Fujiwara,<sup>†</sup> Takeo Otsuka,<sup>†</sup> Hayao Kobayashi,<sup>\*,†</sup> and Mohamedally Kurmoo<sup>\*,⊥</sup>

Institute for Molecular Science and CREST, Japan Science and Technology Corporation, Okazaki 444-8585, Japan, College of Chemistry and Molecular Engineering, Peking University, Beijing 100871, China, Institute of Chemistry, Chinese Academy of Sciences, Beijing 100080, China, Department of Chemistry, Faculty of Science, Hiroshima University, 1-3-1 Kagamiyama, Higashi Hiroshima, Hiroshima 739-8526, Japan, and Laboratoire de Chimie de Coordination Organique, CNRS-UMR 7140, Institut Le Bel, Université Louis Pasteur, 4 rue Blaise Pascal, F-67000 Strasbourg, France

Received June 6, 2006

We report the synthesis, crystal structures, thermal, IR, UV–vis, and magnetic properties of a series of divalent transition metal formates, [NH<sub>4</sub>][M(HCOO)<sub>3</sub>], where M = divalent Mn, Co, or Ni. They crystallize in the hexagonal chiral space group *P*6<sub>3</sub>22. The structure consists of octahedral metal centers connected by the *anti*–*anti* formate ligands, and the ammonium cations sit in the channels. The chiral structure is a framework with the rarely observed 4<sup>9</sup>·6<sup>6</sup> topology, and the chirality is derived from the handedness imposed by the formate ligands around the metals and the presence of units with only one handedness. The thermal properties are characterized by a decomposition at ca. 200 °C. The three compounds exhibit an antiferromagnetic ground state at 8.4, 9.8, and 29.5 K for Mn, Co, and Ni, respectively. The last two display a weak spontaneous magnetization due to a small canting of the moments below the critical temperature, and the Co compound shows a further transition at lower temperatures. The isothermal magnetizations at 2 K show spin-flop fields of 600 Oe (Mn), 14 kOe (Co), and above 50 kOe (Ni) and a small hysteresis with a remnant magnetization of 25 cm<sup>3</sup> G mol<sup>−1</sup> (Co) and 50 cm<sup>3</sup> G mol<sup>−1</sup> (Ni) and coercive field of 400 Oe (Co) and 830 Oe (Ni).

## Introduction

Metal–organic materials with two or more functionalities, e.g., conductivity and magnetism,<sup>1</sup> magnetic and optical properties,<sup>2</sup> porosity and magnetism,<sup>3</sup> and chirality and magnetism,<sup>4–7</sup> currently attract considerable attention because

they provide a good approach to create novel materials with dual functionalities or multifunctionalities and possible interplay between different functions. In this context, chiral

\* To whom correspondence should be addressed. E-mail: hayao@ims.ac.jp (H.K.), zmw@pku.edu.cn (Z.W.), kurmoo@chimie.u-strasbg.fr (M.K.).

<sup>†</sup> Institute for Molecular Science and CREST, Japan Science and Technology Corporation. Fax: 81-564-54-2254.

<sup>‡</sup> Peking University. Fax: 86-10-62751708.

<sup>§</sup> Chinese Academy of Sciences.

<sup>||</sup> Hiroshima University.

<sup>⊥</sup> Université Louis Pasteur.

- (1) (a) Coronado, E.; Galan-Mascarós, J. R.; Gómez-García, C. J.; Laukhin, V. *Nature* **2000**, *408*, 447. (b) Kurmoo, M.; Graham, A. W.; Day, P.; Coles, S. J.; Hursthouse, M. B.; Caulfield, J. L.; Singleton, J.; Pratt, F. L.; Hayes, W.; Ducasse, L.; Guionneau, P. *J. Am. Chem. Soc.* **1995**, *117*, 12209. (c) Coronado, E.; Day, P. *Chem. Rev.* **2004**, *104*, 5419. (d) Uji, S.; Shinagawa, H.; Terashima, T.; Yakabe, T.; Terai, Y.; Tokumoto, M.; Kobayashi, A.; Tanaka, H.; Kobayashi, H. *Nature* **2001**, *410*, 908. (e) Kobayashi, H.; Cui, H.-B.; Kobayashi, A. *Chem. Rev.* **2004**, *104*, 5265.

- (2) (a) Sato, O. *Acc. Chem. Res.* **2003**, *36*, 692. (b) Sunatsuki, Y.; Ikuta, Y.; Matsumoto, N.; Ohta, H.; Kojima, M.; Iijima, S.; Hayami, S.; Maeda, Y.; Kaizaki, S.; Dahan, F.; Tuchagues, J. P. *Angew. Chem., Int. Ed.* **2003**, *42*, 1614. (c) Lacroix, P. G.; Malfant, I.; Bénard, S.; Yu, P.; Rivière, E.; Nakatani, K. *Chem. Mater.* **2001**, *13*, 441. (d) Evans, J. S. O.; Bénard, S.; Yu, P.; Clément, R. *Chem. Mater.* **2001**, *13*, 3813. (3) (a) Maspoch, D.; Ruiz-Molina, D.; Wurst, K.; Domingo, N.; Cavallini, M.; Biscarini, F.; Tejada, J.; Rovira, C.; Veciana, J. *Nat. Mater.* **2003**, *2*, 190. (b) Maspoch, D.; Ruiz-Molina, D.; Veciana, J. *J. Mater. Chem.* **2004**, 2713 and references cited therein. (c) Kurmoo, M.; Kumagai, H.; Chapman, K. W.; Kepert, C. J. *Chem. Commun.* **2005**, 3012. (d) Rujiwatra, A.; Kepert, C. J.; Claridge, J. B.; Rosseinsky, M. J.; Kumagai, H.; Kurmoo, M. *J. Am. Chem. Soc.* **2001**, *123*, 10584. (e) Kurmoo, M.; Kumagai, H.; Hughes, S. M.; Kepert, C. J. *Inorg. Chem.* **2003**, *42*, 6709. (f) Halder, G. J.; Kepert, C. J.; Moubaraki, B.; Murray, K. S.; Cashion, J. D. *Science* **2002**, *298*, 1762. (g) Niel, V.; Thompson, A. L.; Munoz, M. C.; Galet, A.; Goeta, A. E.; Real, J. A., *Angew. Chem., Int. Ed.* **2003**, *42*, 3759. (h) Kepert, C. J. *Chem. Commun.* **2006**, 695.

magnets are of special interest.<sup>4</sup> These materials are not only of academic interests such as asymmetric magnetic anisotropy, magnetic chirality, and magnetochiral dichroism but also have potential for applications as new devices. For most reported chiral magnetic coordination compounds, the chirality of the structure is introduced either by employing enantiopure building blocks, in most case the auxiliary ligands,<sup>4,5</sup> or by spontaneous resolution upon crystallization or other mechanism such as coordination induced chirality from racemic mixture or achiral reaction system.<sup>6,7</sup> To mediate significant magnetic exchange between metal sites short bridging ligands, for example, cyanide,<sup>4,5</sup> azide,<sup>6</sup> and oxalate,<sup>7</sup> are suitable. However, the auxiliary ligands acting as chiral parts are usually so large as to result in both lower framework dimensionality and weak magnetic coupling. From the point of view of magnetism, the auxiliary-ligand-induced chirality, in principle, is not favorable for long-range magnetic ordering because it dilutes the moment carriers and reduces the coupling between these moment carriers in the materials. Therefore, chiral materials with short ligands only are most favorable. While the oxalate systems<sup>8</sup> might be the most promising, new systems need to be explored.

In this work we present a series of chiral, magnetic salts of divalent transition metal formates,  $[\text{NH}_4][\text{M}(\text{HCOO})_3]$ , where  $\text{M} = \text{Mn}$  (**1Mn**),  $\text{Co}$  (**2Co**), and  $\text{Ni}$  (**3Ni**). After quite a long period of silence in the research of molecular magnetism, the formate anion,  $\text{HCOO}^-$ , as the smallest and simplest carboxylate but with all the functionalities of carboxylate ligands, has become attractive again very recently, compared to other popular and small ligands such as cyanide,<sup>4,5,9</sup> azide,<sup>6,10</sup> and oxalate,<sup>7,8,11</sup> having been extensively employed in creating materials with interesting

magnetic properties. The small stereo effect of  $\text{HCOO}^-$  is of benefit for the formation of coordination frameworks, and the short  $\text{HCOO}^-$  bridge, a three- or single-atom connector, is promising for the magnetic coupling between metal sites. The structure and magnetism of metal formate dihydrate salts,  $\text{M}(\text{HCOO})_2 \cdot 2\text{H}_2\text{O}$  ( $\text{M} = \text{Mn}, \text{Fe}, \text{Co}, \text{Ni}, \text{and Cu}$ ),<sup>12</sup> were extensively investigated 30–40 years ago. This isostructural series possesses a 3D framework consisting of layers of (4, 4) net of  $\text{M}(\text{HCOO})_2$  linked by *trans*- $\text{M}(\text{H}_2\text{O})_4(\text{HCOO})_2$  units, and they predominantly exhibit long-range canted antiferromagnetic ordering. In the 1990s other systems of  $\text{M}(\text{HCOO})_2\text{L}_2$ ,<sup>13</sup> where L is a coligand such as urea and formamide, were investigated. They consist also of layers of a (4, 4) net of  $\text{M}(\text{HCOO})_2$  linked by hydrogen bonds, and in some cases, spontaneous magnetization was observed at the Néel transition due to canting of the moments. Combining  $\text{HCOO}^-$  and other ditopic ligands to build magnetic coordination polymers has only recently been realized and has led to the realization that formate ligand behaves quite similar to azide in coordination.<sup>14</sup> Transition metal formates without coligands are very limited, and several novel binary systems have recently been added to this list, except some known  $\text{Ca/Sr-Cu}$  formate salts.<sup>15</sup> Examples include ferromagnetic  $\alpha\text{-Cu}(\text{HCOO})_2$  having a 3D-framework and  $\beta\text{-Cu}(\text{HCOO})_2$  having an infinite chain structure,<sup>16</sup> an anhydrous  $\text{Mn}(\text{HCOO})_2$  with a structure topologically related to  $\text{Mn}(\text{HCOO})_2 \cdot 2\text{H}_2\text{O}$ , which orders as an antiferromagnet at 8 K,<sup>17</sup> and the porous  $[\text{M}_3(\text{HCOO})_6]$  family ( $\text{M} = \text{Mn}, \text{Fe}, \text{Co}, \text{Ni}, \text{and Zn}$ , as well as non-

- (4) Inoue, K.; Ohkoshi, S. I.; Imai, H. In *Magnetism: Molecules to Materials V*; Miller, J. S., Drillon, M., Eds.; Wiley-VCH Verlag GmbH & Co. KGaA: Weinheim, Germany, 2005; Chapter 2.
- (5) (a) Imai, H.; Inoue, K.; Kikuchi, K.; Yoshida, Y.; Ito, M.; Sunahara, T.; Onaka, S. *Angew. Chem., Int. Ed.* **2004**, *43*, 5618. (b) Inoue, K.; Kikuchi, K.; Ohba, M.; Okawa, H. *Angew. Chem., Int. Ed.* **2003**, *42*, 4810.
- (6) (a) Coronado, E.; Galán-Mascarós, J. R.; Gómez-García, C. J.; Martínez-Ferrero, M.; Almeida, M.; Waerenborgh, J. C. *Eur. J. Inorg. Chem.* **2005**, 2064. (b) Gao, E. Q.; Yue, Y. F.; Bai, S. Q.; He, Z.; Yan, C.-H. *J. Am. Chem. Soc.* **2004**, *126*, 1419.
- (7) (a) Gruselle, M.; Thouvenot, R.; Malézieux, B.; Train, C.; Gredin, P.; Demeschik, T. V.; Troitskaya, L. L.; Sokolov, V. I. *Chem.—Eur. J.* **2004**, *10*, 4763. (b) Coronado, E.; Galán-Mascarós, J. R.; Gómez-García, C. J.; Martínez-Agudo, J. M. *Inorg. Chem.* **2001**, *40*, 113. (c) Andrés, R.; Brissard, M.; Gruselle, M.; Train, C.; Vaissermann, J.; Malézieux, B.; Jamet, J. P.; Verdager, M. *Inorg. Chem.* **2001**, *40*, 4633.
- (8) (a) Clément, R.; Decurtins, S.; Gruselle, M.; Train, C. *Monatsh. Chem.* **2003**, *134*, 117. (b) Coronado, E.; Galán-Mascarós, J. R.; Gómez-García, C. J.; Martínez-Agudo, J. M. *Adv. Mater.* **1999**, *11*, 558.
- (9) For reviews, see the following: (a) Ohba, M.; Okawa, H. *Coord. Chem. Rev.* **2000**, *198*, 313. (b) Miller, J. S.; Manson, J. L. *Acc. Chem. Res.* **2001**, *34*, 563. (c) Lescouëzec, R.; Toma, L. M.; Vaissermann, J.; Verdager, M.; Delgado, F. S.; Ruiz-Pérez, C.; Lloret, F.; Julve, M. *Coord. Chem. Rev.* **2005**, *249*, 2691.
- (10) For example, see the following: (a) Ribas, J.; Escuer, A.; Monfort, M.; Vicente, R.; Cortés, R.; Lezama, L.; Rojo, T. *Coord. Chem. Rev.* **1999**, *193–195*, 1027. (b) Hong, C. S.; Do, Y. *Angew. Chem., Int. Ed.* **1999**, *38*, 193. (c) Han, S.; Manson, J. L.; Kim, J.; Miller, J. S. *Inorg. Chem.* **2000**, *39*, 4182. (d) Liu, T. F.; Fu, D.; Gao, S.; Zhang, Y. Z.; Sun, H. L.; Su, G.; Liu, Y. J. *J. Am. Chem. Soc.* **2003**, *125*, 13976. (e) Zhang, Y. Z.; Wei, H. Y.; Pan, F.; Wang, Z. M.; Chen, Z. D.; Gao, S. *Angew. Chem., Int. Ed.* **2005**, *44*, 5841. (f) Zhang, Y. Z.; Gao, S.; Sun, H. L.; Su, G.; Wang, Z. M.; Zhang, S. W. *Chem. Commun.* **2004**, 1906.
- (11) (a) Rao, C. N. R.; Natarajan, S.; Vaidyanathan, R. *Angew. Chem., Int. Ed.* **2004**, *43*, 1466. (b) Tamaki, H.; Zhong, Z. H.; Matsumoto, N.; Kida, S.; Koikawa, K.; Achiwa, N.; Okawa, H. *J. Am. Chem. Soc.* **1992**, *114*, 6974. (c) Mathoniere, C.; Nuttall, C. J.; Carling, S. G.; Day, P. *Inorg. Chem.* **1996**, *35*, 1201. (d) Decurtins, S.; Schmalke, H. W.; Schneuwly, O.; Ensling, J.; Gutlich, P. *J. Am. Chem. Soc.* **1994**, *116*, 9521.
- (12) (a) Osaki, K.; Nakai, Y. *J. Phys. Soc. Jpn.* **1963**, *18*, 919. (b) Osaki, K.; Nakai, Y.; Watanabe, T. *J. Phys. Soc. Jpn.* **1964**, *19*, 717. (c) Abe, H.; Morigaki, H.; Matsuura, M.; Torii, K.; Yamagata, K. *J. Phys. Soc. Jpn.* **1964**, *19*, 775. (d) Abe, H.; Torii, K. *J. Phys. Soc. Jpn.* **1965**, *20*, 183. (e) Yamagata, K.; Abe, H. *J. Phys. Soc. Jpn.* **1965**, *20*, 906. (f) Yamagata, K. *J. Phys. Soc. Jpn.* **1967**, *22*, 582. (g) Pierce, R. D.; Friedberg, S. A. *Phys. Rev.* **1968**, *165*, 680. (h) Skalyo, J., Jr.; Shirane, G.; Friedberg, S. A. *Phys. Rev.* **1969**, *188*, 1037. (i) Takeda, K.; Kawasaki, K. *J. Phys. Soc. Jpn.* **1971**, *31*, 1026. (j) Radhakrishna, P.; Gillon, B.; Chevrier, G. *J. Phys.: Condens. Matter* **1993**, *5*, 6447. (k) Hoy, G. R.; Barros, S. de S.; Barros, F. de S.; Friedberg, S. A. *J. Appl. Phys.* **1965**, *36*, 936. (l) Pierce, R. D.; Friedberg, S. A. *Phys. Rev.* **1971**, *B3*, 934. (m) Takeda, K.; Matsukawa, S. i. *J. Phys. Soc. Jpn.* **1971**, *30*, 887. (n) Flippen, R. B.; Friedberg, S. A. *J. Chem. Phys.* **1963**, *38*, 2652. (o) Kobayashi, H.; Haseda, T. *J. Phys. Soc. Jpn.* **1963**, *18*, 541. (p) Martin, R. L.; Waterman, H. *J. Chem. Soc.* **1959**, 1359.
- (13) (a) Ridwan, *Jpn. J. Appl. Phys.* **1992**, *31*, 3559 and references cited therein. (b) Rettig, S. J.; Thompson, R. C.; Trotter, J.; Xia, S. H. *Inorg. Chem.* **1999**, *38*, 1360.
- (14) (a) Manson, J. L.; Lecher, J. G.; Gu, J.; Geiser, U.; Schlueter, J. A.; Hennig, R.; Wang, X.; Schultz, A. J.; Koo, H. J.; Whangbo, M. H. *Dalton Trans.* **2003**, 2905. (b) Wang, X. Y.; Wei, H. Y.; Wang, Z. M.; Chen, Z. D.; Gao, S. *Inorg. Chem.* **2005**, *44*, 572.
- (15) (a) Sanchis, M. J.; Gómez-Romero, P.; Folgado, J. V.; Sapiña, F.; Ibáñez, R.; Beltrán, A.; García, J.; Beltrán, D. *Inorg. Chem.* **1992**, *31*, 2915. (b) Levya, A. G.; Polla, G.; de Perazzo, P. K.; Lanza, H.; de Benyacar, M. A. R. *J. Solid State Chem.* **1996**, *123*, 291. (c) Polla, G.; Levya, G.; de Perazzo, P. K.; Lanza, H.; de Benyacar, M. A. R. *J. Solid State Chem.* **1995**, *117*, 145.
- (16) Sapiña, F.; Burgos, M.; Escrivá, E.; Folgado, J.-V.; Marcos, D.; Beltrán, A.; Beltrán, D. *Inorg. Chem.* **1993**, *32*, 4337.
- (17) Viertelhaus, M.; Henke, H.; Anson, C. E.; Powell, A. K. *Eur. J. Inorg. Chem.* **2003**, 2283.

transition-metal  $\text{Mg}^{18-21}$  possessing an unusual diamond open framework and showing a wide spectrum of guest inclusion. In this family the Mn and Fe members have been proved to exhibit long-range magnetic ordering and guest modulated Curie temperature.<sup>18</sup> Enlightened by a 3D NaCl-type framework of  $\text{Mn}^{\text{III}}(\text{HCOO})_3$ ,<sup>22</sup> reported in 1999, with carbon dioxide and/or formic acid guests in the cavities, the fact that many known divalent metal formates<sup>12,13</sup> have layers of a (4, 4) net, and the cation template effect exhibited in cyanide, azide, and dicyanamide 3D NaCl-type systems,<sup>23</sup> we and other authors have successfully obtained NaCl-type frameworks of  $[\text{M}^{\text{II}}(\text{HCOO})_3]^-$  in series of a perovskite compounds of  $[\text{AmineH}^+][\text{M}(\text{HCOO})_3]^-$ ,<sup>24</sup> when protonated amine cations,  $\text{AmineH}^+ = \text{CH}_3\text{NH}_3^+$ ,  $(\text{CH}_3)_2\text{NH}_2^+$ ,  $\text{CH}_3\text{-CH}_2\text{NH}_3^+$ , and  $(\text{CH}_2)_3\text{NH}_2^+$ , possessing about 3 non-hydrogen atoms, as well as non-coordinating solvent, were employed.<sup>24b</sup> However, employment of a bulky  $\text{AmineH}^+$  such as  $(\text{CH}_3\text{CH}_2)_3\text{NH}^+$ ,  $(\text{CH}_3\text{CH}_2)_2\text{NH}_2^+$ , or  $\text{CH}_3\text{CH}_2\text{CH}_2\text{-NH}_3^+$  resulted in the porous  $[\text{M}_3(\text{HCOO})_6]$ .<sup>18,19,20b</sup> The question is thus opened to what will happen if the smallest ammonium  $\text{NH}_4^+$  is used. We here report the outcome, where the chiral magnetic salts  $[\text{NH}_4][\text{M}(\text{HCOO})_3]$  were isolated. It is interesting to see the appearance of chirality from these simple achiral starting materials. The structure is a framework with rarely observed  $4^9\cdot6^6$  topology, consisting of octahedral metal centers connected by *anti-anti* formate ions and the ammonium cation arrays located in the channels. **1Mn** is an antiferromagnet, exhibiting spin-flop field at very low field, while both **2Co** and **3Ni** are weak ferromagnets and **2Co** displays possible spin-reorientation after the antiferromagnetic ordering. Thermal and spectroscopic properties are also investigated.

## Experimental Section

**Synthesis.** All starting chemicals were commercially available reagents of analytical grade and used without further purification.

- (18) (a) Wang, Z. M.; Zhang, B.; Fujiwara, H.; Kobayashi, H.; Kurmoo, M. *Chem. Commun.* **2004**, 416. (b) Zhang, B.; Wang, Z. M.; Kurmoo, M.; Gao, S.; Inoue, K.; Kobayashi, H. *Adv. Funct. Mater.* **2007**, in press. (c) Wang, Z. M.; Zhang, Y. J.; Liu, T.; Kurmoo, M.; Gao, S. *Adv. Funct. Mater.* **2007**, in press.
- (19) Wang, Z. M.; Zhang, B.; Kurmoo, M.; Green, M. A.; Fujiwara, H.; Otsuka, T.; Kobayashi, H. *Inorg. Chem.* **2005**, *44*, 1230.
- (20) (a) Viertelhaus, M.; Adler, P.; Clérac, R.; Anson, C. E.; Powell, A. K. *Eur. J. Inorg. Chem.* **2005**, 692. (b) Wang, Z. M.; Zhang, Y. J.; Kurmoo, M.; Liu, T.; Vilminot, S.; Zhao, B.; Gao, S. *Aust. J. Chem.* **2006**, *59*, 617.
- (21) (a) Dybtsev, D. N.; Chun, H.; Yoon, S. H.; Kim, D.; Kim, K. *J. Am. Chem. Soc.* **2004**, *126*, 32. (b) Rood, J. A.; Noll, B. C.; Henderson, K. W. *Inorg. Chem.* **2006**, *45*, 5521.
- (22) Cornia, A.; Caneschi, A.; Dapporto, P.; Fabretti, A. C.; Gatteschi, D.; Malavasi, W.; Sangregorio, C.; Sessoli, R. *Angew. Chem., Int. Ed.* **1999**, *38*, 1780.
- (23) (a) Entley, W. R.; Girolami, G. S. *Inorg. Chem.* **1994**, *33*, 5165. (b) Sato, O.; Iyoda, T.; Fujishima, A.; Hashimoto, K. *Science* **1996**, *271*, 49. (c) Ferlay, S.; Mallah, T.; Ouahès, R.; Veillet, P.; Verdager, M. *Nature* **1995**, *378*, 701. (d) Ferlay, S.; Mallah, T.; Ouahès, R.; Veillet, P.; Verdager, M. *Inorg. Chem.* **1999**, *38*, 229. (e) Dong, W.; Zhu, L. N.; Song, H. B.; Liao, D. Z.; Jiang, Z. H.; Yan, S. P.; Cheng, P.; Gao, S. *Inorg. Chem.* **2004**, *43*, 2465. (f) Mautner, F. A.; Cortés, R.; Lezama, L.; Rojo, T. *Angew. Chem., Int. Ed.* **1996**, *35*, 78. (h) Tong, M. L.; Ru, J.; Wu, Y. M.; Chen, X. M.; Chang, H. C.; Mochizuki, K.; Kitagawa, S. *New J. Chem.* **2003**, *27*, 779.
- (24) (a) Wang, X. Y.; Gan, L.; Zhang, S. W.; Gao, S. *Inorg. Chem.* **2004**, *43*, 4615. (b) Wang, Z. M.; Zhang, B.; Otsuka, T.; Inoue, K.; Kobayashi, H.; Kurmoo, M. *Dalton Trans.* **2004**, 2209.

$[\text{NH}_4][\text{M}(\text{HCOO})_3]$  ( $\text{M} = \text{Mn}$  (**1Mn**),  $\text{Co}$  (**2Co**), and  $\text{Ni}$  (**3Ni**)) were obtained by the reaction of the metal chloride with  $[\text{NH}_4][\text{HCOO}]$  from formic acid neutralized by ammonia in methanol. For **1Mn**, 10 mL of methanol solution containing 203 mg of  $\text{MnCl}_2\cdot 4\text{H}_2\text{O}$  was mixed with 5.5 mL of methanol solution of 0.80 M  $[\text{NH}_4][\text{HCOO}]$  (prepared by mixing 2.7 g of 25% aqueous  $\text{NH}_3\cdot\text{H}_2\text{O}$  and 2.4 g of  $\text{HCOOH}$  in 50 mL of methanol with pH  $\sim 5$ ). The mixed solution was kept undisturbed. Pale pink hexagonal bipyramid shaped crystals were harvested after 1 day. The crystals were washed with methanol and dried under vacuum. The yield is 72% based on Mn. However, **2Co** and **3Ni** were prepared via a carefully applied slow diffusion method due to their lower solubilities. For **2Co**, 5 mL of methanol solution containing 0.80 M  $[\text{NH}_4][\text{HCOO}]$  was placed at the bottom of a glass tube (6 mm inner diameter). On the  $[\text{NH}_4][\text{HCOO}]$  solution, 4 mL of methanol was gently added, followed by carefully layering 5 mL of methanol solution of 0.20 M  $\text{CoCl}_2\cdot 6\text{H}_2\text{O}$ . The tube was sealed and kept undisturbed. Violet-red, hexagonal bipyramid-shaped crystals were harvested after 5 days. The yield is 90% based on the starting cobalt salt. The product was washed with methanol and dried in vacuum. A similar procedure employing  $\text{NiCl}_2\cdot 6\text{H}_2\text{O}$  instead of the  $\text{CoCl}_2\cdot 6\text{H}_2\text{O}$  took 10 days of crystallization to produce green crystals of **3Ni** in a yield of 42%, and the crystal shape was found to be similar to that of **1Mn** and **2Co**. Anal. Calcd for **1Mn**,  $\text{C}_3\text{H}_7\text{NO}_6\text{Mn}$ : C, 17.32; H, 3.39; N, 6.73. Found: C, 17.11; H, 3.30; N, 6.68. Calcd for **2Co**,  $\text{C}_3\text{H}_7\text{NO}_6\text{Co}$ : C, 16.99; H, 3.33; N, 6.61. Found: C, 16.84; H, 3.26; N, 6.49. Calcd for **3Ni**,  $\text{C}_3\text{H}_7\text{NO}_6\text{Ni}$ : C, 17.01; H, 3.33; N, 6.61. Found: C, 16.99; H, 3.38; N, 6.37.

**X-ray Crystallography.** The crystallographic data for the single crystals of the three compounds were collected at room temperature on a Rigaku AFC7 Mercury CCD diffractometer with 5.4 kW rotating anode source using graphite-monochromated  $\text{Mo K}\alpha$  radiation of  $\lambda = 0.71073 \text{ \AA}$ .<sup>25</sup> The structures were solved by direct methods and refined by full-matrix least-squares on  $F^2$  using the SHELX program.<sup>26</sup> The H atoms were located from the difference Fourier synthesis, and refined isotropically. The refined C/N–H distances, bond angles involving H atoms, and isotropic thermal factors of H atoms are all of rational values. The tetrahedral  $\text{NH}_4^+$  cation showed a trigonal disorder but has a well-defined unique H atom in the structure solution and refinement. The details of data collection, data reduction, and crystallographic data are summarized in Table 1. Powder XRD patterns of the three compounds were obtained on a Rigaku RINT2000 diffractometer at room temperature with  $\text{Cu K}\alpha$  radiation in a flat plate geometry.

**Physical Measurements.** Dc and ac magnetization measurements were performed on three different Quantum Design SQUID systems, MPMS7EB, MPMS5S, and MPMS2, for polycrystalline samples tightly sealed in Al foil. Diamagnetic corrections were estimated using Pascal constants<sup>27</sup> ( $-78 \times 10^{-6}$ ,  $-76 \times 10^{-6}$ , and  $-74 \times 10^{-6} \text{ cm}^3\text{mol}^{-1}$  for **1Mn**, **2Co**, and **3Ni**, respectively) and background correction by experimental measurement on neat Al foil. Thermal analyses, TGA and DSC, were performed on a SDT 2960 thermal analyzer and a DSC 2010 differential scanning calorimeter at  $5^\circ\text{C}/\text{min}$  under  $\text{N}_2$ . FTIR spectra were recorded using pure samples in the range of  $4000$  to  $650 \text{ cm}^{-1}$  on a Nicolet Magna 750 FT/IR spectrometer. UV–vis spectra of **1Mn**, **2Co**, and **3Ni** were recorded on a Shimadzu UV-VIS-3100 spectrophotometer with an

(25) CrystalClear software; Rigaku Corp.: Tokyo, Japan, 2000.

(26) Sheldrick, G. M. *SHELX-97, Program for Crystal Structure Determination*; University of Göttingen: Göttingen, Germany, 1997.

(27) Mulay, L. N.; Boudreaux, E. A. *Theory and Applications of Molecular Diamagnetism*; John Wiley & Sons Inc.: New York, 1976.



**Table 1.** Crystallographic Data for **1Mn**, **2Co**, and **3Ni**

	<b>1Mn</b>	<b>2Co</b>	<b>3Ni</b>
formula	C <sub>3</sub> H <sub>7</sub> MnNO <sub>6</sub>	C <sub>3</sub> H <sub>7</sub> CoNO <sub>6</sub>	C <sub>3</sub> H <sub>7</sub> NiNO <sub>6</sub>
fw	208.04	212.03	211.81
<i>T</i> , K	293	293	293
crystal system	hexagonal	hexagonal	hexagonal
space group	<i>P</i> 6 <sub>3</sub> 22	<i>P</i> 6 <sub>3</sub> 22	<i>P</i> 6 <sub>3</sub> 22
<i>a</i> , Å	7.356(2)	7.297(2)	7.286(1)
<i>b</i> , Å	7.356(2)	7.297(2)	7.286(1)
<i>c</i> , Å	8.478(2)	8.179(2)	8.021(2)
α, deg	90	90	90
β, deg	90	90	90
γ, deg	120	120	120
<i>V</i> , Å <sup>3</sup>	397.3(1)	377.1(2)	368.8(1)
<i>Z</i>	2	2	2
<i>D</i> <sub>c</sub> , g/cm <sup>3</sup>	1.739	1.867	1.908
μ(Mo Kα), mm <sup>−1</sup>	1.648	2.261	2.616
crystal size, mm <sup>3</sup>	0.11 × 0.10 × 0.09	0.15 × 0.15 × 0.10	0.15 × 0.13 × 0.09
<i>T</i> <sub>min</sub> and <i>T</i> <sub>max</sub>	0.882, 1.000	0.884, 1.000	0.879, 1.000
θ <sub>min</sub> , θ <sub>max</sub> , deg	3.20, 27.46	4.99, 27.41	4.11, 27.45
no. of total reflections	6804	6296	6201
no. of unique reflections ( <i>R</i> <sub>int</sub> )	313 (0.0378)	297 (0.0288)	280 (0.0294)
no. of observed [ <i>I</i> ≥ 2σ( <i>I</i> )]	291	285	251
no. of parameters	26	26	25
<i>R</i> 1, <i>wR</i> 2 [ <i>I</i> ≥ 2σ( <i>I</i> )]	0.0195, 0.0441	0.0157, 0.0413	0.0168, 0.0418
<i>R</i> 1, <i>wR</i> 2 (all data)	0.0216, 0.0443	0.0166, 0.0415	0.0180, 0.0421
GOF	1.152	1.192	1.172
Flack parameters	0.01(4)	0.02(3)	0.01(4)
Δρ, <sup>a</sup> e/Å <sup>3</sup>	0.153, −0.189	0.141, −0.194	0.210, −0.228
max and mean Δ/σ <sup>b</sup>	0.000, 0.000	0.000, 0.000	0.000, 0.000

<sup>a</sup> Max and min residual density. <sup>b</sup> Max and mean shift/sigma.

integrated sphere attachment in the range 200–1000 nm on ground powder samples referenced to a BaSO<sub>4</sub> background.

## Results and Discussion

### Synthesis and the Role of Protonated Amine Cations.

During our systematic investigation of the cation-template effect<sup>18,19,24b</sup> on the formation of 3d metal formate frameworks, we have examined the smallest ammonium cation, NH<sub>4</sub><sup>+</sup>. In this work the three compounds [NH<sub>4</sub>][M(HCOO)<sub>3</sub>] (M = Mn, Co, and Ni) were prepared by the reaction of divalent metal chlorides with formic acid neutralized by ammonia in methanol. This work emphasizes the conclusion drawn in previous reports where we demonstrate the role of protonated amine cations of different size in controlling the type of metal–formate framework.<sup>19,24b</sup> When large or bulky amines such as triethylamine, diethylamine, or propylamine are used, the products are the nanoporous diamond framework compounds [M<sub>3</sub>(HCOO)<sub>6</sub>]*·*solvent (M = divalent Mn, Fe, Co, Ni, and Zn), with open channels occupied by solvents.<sup>18,19,20b</sup> The solvents are easily removed to leave a stable framework with free space which can be refilled with other guests. The use of amines of middle size with 2–4 non-H atoms (methylamine, dimethylamine, ethylamine, and cyclotrimethyleneamine) results in the perovskite compounds [AmineH<sup>+</sup>][M(HCOO)<sub>3</sub>] (M = divalent Fe, Mn, Co, Ni, Cu, and Zn)<sup>24b</sup> having a NaCl-like anionic metal–formate framework incorporating the ammonium cations within the cavities. The smallest ammonium used in this work produces a hexagonal variety of metal–formate frameworks, [NH<sub>4</sub>][M(HCOO)<sub>3</sub>] (M = Mn, Co, and Ni), where the NH<sub>4</sub><sup>+</sup> cations occupy hexagonal channels and the framework topology is

the rare 4<sup>9</sup>·6<sup>6</sup> one<sup>28,29</sup> that is different from the NaCl-like one (see structure discussion later). While the smaller protonated amine cations are found to coexist with the metal–formate frameworks, the bulky ones are absent in the final frameworks. This is because the metal–formate frameworks with the short HCOO ligand are unable to accommodate the large protonated amine cations. Therefore, we can reach the conclusion that the size of protonated amine cations controls the structures of the final metal–formate frameworks. In addition, it is worth noting that the use of noncoordinating solvent such as methanol as the major solvent is another key requirement to obtain these metal formates without coligands because it inhibits the formation of metal–formates with coordinated ligands, as what was observed for many known metal formates.<sup>12,13</sup> Finally, the PXRD patterns of the three compounds revealed that they are single phase products, as shown in Figure S1 (Supporting Information).

**Crystal Structure.** The three compounds are isomorphs and belong to the chiral hexagonal space group *P*6<sub>3</sub>22 (Table 1). The structure is an unusual 3D anionic [M(HCOO)<sub>3</sub>]<sup>−</sup> framework (Figures 1 and S2) displaying hexagonal channels along the *c*-axis in which the NH<sub>4</sub><sup>+</sup> cations are located. In the framework, each octahedral (MO<sub>6</sub>) metal ion is connected to six neighboring metal ions via bridging HCOO groups adopting the *anti*–*anti* mode; thus, it is a 6-connected node (Figure S2a). The framework can be considered as (4, 4) sheets along the *a* direction linked along the *b* direction

- (28) (a) Wells, A. F. *Three-Dimensional Nets and Polyhedra*; Wiley-Interscience: New York, 1977. (b) Wells, A. F. *Further Studies of Three-dimensional Nets*; American Crystallographic Association: Pittsburgh, PA, 1979 (distributed by Polycrystal Book Service).  
 (29) Batten, S. R.; Robson, R. *Angew. Chem., Int. Ed.* **1998**, 37, 1460.

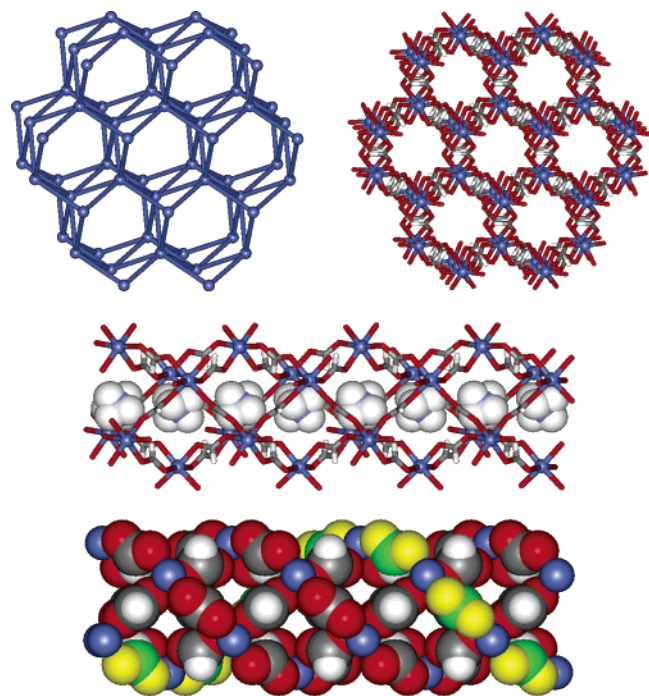


**Figure 1.** Structure of chiral salts of  $[\text{NH}_4][\text{M}(\text{HCOO})_3]$ , with **2Co** as the representative: top left, the topological view where spheres are Co atoms and bonds the *anti-anti* HCOO linkages; top right, the hexagonal framework of  $[\text{NH}_4][\text{Co}(\text{HCOO})_3]$  with  $\text{NH}_4^+$  cations in channels omitted; middle, one channel with trigonally disordered  $\text{NH}_4^+$  cation array inside, highlighted in a space-filling model; bottom, the helical characteristics of the channel, a triplet helix with a pitch of  $3 \times c$ . One helix (with C–H toward inside the channel) is highlighted by green C and yellow O atoms. The helices are further cross-linked by HCOO groups with C–H toward outside the channel. This linkage creates other groups of triplet helices but with the C–H toward the outside of the channel. Colors for coding atoms: H, white; C, gray and green; O, red and yellow; Co, blue.

or vice versa, or the same (4, 4) sheets along  $a + b$  linked along  $a - b$ , with the intersheet linkage in a zigzag style. In fact, the framework is the three equivalent sets of the (4, 4) sheet, parallel to the  $a$ ,  $b$  and  $a + b$  directions, merged together. Since there is one unique 6-connected node in the framework and there are nine 4-gons and six 6-gons (the small circuits) around each node, the topology of the 3D framework is therefore  $4^9 \cdot 6^6$  using the Schafli symbol (Figure 1, top left).<sup>28,29</sup> This is unlike the recently reported perovskite or NaCl frameworks,  $[\text{AmineH}^+][\text{M}(\text{HCOO})_3]$ ,<sup>24</sup> which has the  $4^{12} \cdot 6^3$  topology. The  $4^9 \cdot 6^6$  topology is rarely observed in coordination polymers, and probably the only known example is  $[\text{Eu}(\text{Ag}(\text{CN})_2)_3(\text{H}_2\text{O})_3]$  where the nodes are trigonal prismatic Eu sites and the connections are Eu–NC–Ag–CN–Eu linkages.<sup>29,30</sup> The sides of each hexagonal channel of  $[\text{NH}_4][\text{M}(\text{HCOO})_3]$  are composed of zigzag M–O–CH–O–M links (Figure 1, middle). The chirality of the framework, originating from the presence of only one enantiomer  $\text{M}(\text{OCO})_6$  (Figure S2a), results in the helical channels (Figure 1, bottom). The framework is a bidirectional, triple helix with a pitch of  $3 \times c$  and repeat unit of 6 metal ions. It is interesting to observe the formation of a chiral network from the simple achiral components ( $\text{NH}_4^+$ ,  $\text{M}^{2+}$ , and  $\text{HCOO}^-$ ) as that observed in simple systems such

as  $\text{NaClO}_3$ , quartz, and urea inclusion compounds.<sup>31</sup> The channels having a diameter of 3.1 Å not including the van der Waals radii of the surface atoms (Figure S2c) are occupied by  $\text{NH}_4^+$  cations in a linear array (Figure 1, middle, and Figure S2b). The ammonium shows trigonal disorder and N–H...O hydrogen bonds to the anionic framework (Table 2). It is clear that the  $\text{NH}_4^+$  not only balances the charge but also plays a template role in the formation of this particular  $[\text{M}^{\text{II}}(\text{HCOO})_3]^-$  framework. The decreases in the unique M–O distances of 2.186, 2.101, and 2.064 Å (Table 2), for **1Mn**, **2Co**, and **3Ni**, respectively, are in good agreement with the decrease in the ionic radii in the sequence  $\text{Mn}^{2+}$  (0.97 Å),  $\text{Co}^{2+}$  (0.89 Å), and  $\text{Ni}^{2+}$  (0.83 Å),<sup>32</sup> as well as to those in other metal–formates.<sup>12,13,24a</sup> Consequently, a systematic contraction of the lattice parameters (Table 1) and M...M distances via bridging  $\text{HCOO}^-$ , being 6.000, 5.871, and 5.812 Å for **1Mn**, **2Co**, and **3Ni**, respectively, is observed. The bond angles around the metal sites (Table 2) characterize the distortion of the  $\text{MO}_6$  octahedra. It is worth pointing out that there is no center of symmetry between metal sites bridged by  $\text{HCOO}^-$ , and each coordination octahedron of metal ion has a different orientation from its six neighbors. This provides the possibility of the Dzyaloshinsky–Moriya interaction<sup>33</sup> between magnetic metal sites, as for many metal–formates.<sup>12,13,14b,24</sup>

**IR and UV–Vis Spectra and Thermal Properties.** The IR and UV–vis absorption bands in the spectra and their assignments for the three compounds are given in Table 3. The IR spectra of the three compounds are almost the same (Table 3 and Figure S3), with characteristic bands for the  $\text{NH}_4^+$  ion and the  $\text{HCOO}^-$  group,<sup>34</sup> reflecting the fact that the three structures are the same, these bands being coincident with those previously reported.<sup>17,24b,35</sup> The UV–vis absorption bands (Table 3 and Figure S4) are typical for octahedral  $\text{M}^{2+}$  ions and very similar to that of  $\text{M}(\text{H}_2\text{O})_6^{2+}$ .<sup>36</sup> The strong absorption in the visible region of the chiral magnetic salts of **2Co** and **3Ni** makes them possible candidates for further magneto–optical study.

The thermal properties of the three compounds were investigated by TGA/DSC under nitrogen atmosphere (Figure S5). **1Mn** and **2Co** show two well-defined weight losses while **3Ni** displayed only one with a percentage corresponding to roughly the sum of the two for **1Mn** and **2Co**. For

- (31) (a) McBride, J. M.; Carter, R. L. *Angew. Chem., Int. Ed.* **1991**, *30*, 293. (b) Cotton, F. A.; Wilkinson, G. C.; Murillo, A.; Bochmann, M. *Advanced Inorganic Chemistry*, 6th ed.; John Wiley & Sons, Inc.: New York, 1999; p 273. (c) Hollingsworth M. D.; Harris, K. D. M. In *Comprehensive Supramolecular Chemistry Vol. 6, Solid-State Supramolecular Chemistry: Crystal Engineering*; MacNical, D. D., Toda, F., Bishop, R., Eds.; Pergamon Elsevier Science Ltd.: Oxford, U.K., 1996; pp 178–182.
- (32) Cotton, F. A.; Wilkinson, G. C.; Murillo, A.; Bochmann, M. *Advanced Inorganic Chemistry*, 6th ed.; John Wiley & Sons, Inc.: New York, 1999; p 1304.
- (33) (a) Dzyaloshinsky, I. *J. Phys. Chem. Solid* **1958**, *4*, 241. (b) Moriya, T. *Phys. Rev.* **1960**, *120*, 91. (c) Moriya, T. In *Magnetism Vol. 1*; Rado, G. T., Suhl, H., Eds.; Academic Press: New York, 1963; pp 85–124.
- (34) Nakamoto, K. *Infrared and Raman Spectra of Inorganic and Coordination Compounds*; Wiley: New York, 1986.
- (35) Stoilova, D.; Koleva, V. *J. Mol. Struct.* **2000**, *553*, 131.
- (36) Figgis, B. N.; Hitchman, M. A. *Ligand Field Theory and Its Application*; Wiley-VCH: New York, 2000; p 205.

(30) Assefa, Z.; Staples, R. J.; Fackler, J. P., Jr. *Acta. Crystallogr., Sect. C* **1995**, *51*, 2527.

**Table 2.** Unique Bond Distances (Å) and Angles (deg) and N/C–H···O Hydrogen Bonds (Å, deg) Observed in **1Mn**, **2Co**, and **3Ni**

	<b>1Mn</b> <sup>a</sup>	<b>2Co</b> <sup>b</sup>	<b>3Ni</b> <sup>b</sup>
M(1)–O(1)	2.186(1)	2.101(1)	2.064(1)
C(1)–O(1)	1.235(2)	1.240(2)	1.238(2)
O(1)–M(1)–O(1) <sup>#1</sup>	82.29(6)	82.53(6)	82.64(7)
O(1)–M(1)–O(1) <sup>#2</sup>	96.94(6)	95.28(6)	94.56(7)
O(1)–M(1)–O(1) <sup>#3</sup>	90.85(4)	91.44(4)	91.70(5)
O(1) <sup>#2</sup> –M(1)–O(1) <sup>#3</sup>	169.67(6)	171.07(6)	171.67(7)
M(1)–O(1)–C(1)	123.3(1)	123.3(1)	123.6(2)
O(1)–C(1)–O(1) <sup>#4</sup>	127.2(3)	125.9(2)	125.9(3)

	D–H···A	d(D–H)	d(H···A)	d(D···A)	<(DHA)
<b>1Mn</b> <sup>a</sup>	N(1)–H(2)···O(1)	0.97(2)	2.03(2)	2.972(1)	163(2)
	C(1)–H(1)···O(1) <sup>#5</sup>	1.12(5)	2.42(2)	3.127(3)	119(1)
<b>2Co</b> <sup>b</sup>	N(1)–H(2)···O(1)	0.96(2)	2.06(2)	2.976(1)	159(2)
	C(1)–H(1)···O(1) <sup>#5</sup>	1.07(3)	2.39(2)	3.039(2)	117.3(7)
<b>3Ni</b> <sup>c</sup>	N(1)–H(2)···O(1)	1.04(4)	2.07(5)	2.986(1)	146(3)
	C(1)–H(1)···O(1) <sup>#5</sup>	0.98(4)	2.42(2)	3.006(2)	118.1(8)

<sup>a</sup> Symmetry codes: #1  $-y + 1, -x + 1, -z + 1/2$ ; #2  $x, x - y + 1, -z + 1/2$ ; #3  $-x + y, -x + 1, z$ ; #4  $-x, -x + y, -z$ ; #5  $-y + 1, x - y + 1, z$ .

<sup>b</sup> Symmetry codes: #1  $-y + 1, -x + 1, -z + 3/2$ ; #2  $x, x - y, -z + 3/2$ ; #3  $-x + y + 1, -x + 1, z$ ; #4  $-x + 2, -x + y + 1, -z + 2$ ; #5  $-y + 1, x - y, z$ . <sup>d</sup> The difference in symmetry codes in this table arose from the different absolute configuration of the chiral crystal structures, where **2Co** and **3Ni** are the same while **1Mn** is different.

**Table 3.** IR and UV–Vis Absorption Bands (cm<sup>−1</sup>) and Their Assignments for **1Mn**, **2Co**, and **3Ni**<sup>a</sup>

IR				
assignments	<b>1Mn</b>	<b>2Co</b>	<b>3Ni</b>	
$\nu(\text{NH}_4^+)$ : $\nu_1 + \nu_5$ ( $\nu_5$ , lattice mode)	3330 sh	3335 sh	3333 sh	
$\nu_3$	3167 m	3171 m	3182 m	
$\nu_1$ or $\nu_2 + \nu_4$	3000 m, br	2995 m, br	3000 m, br	
$2\nu_4$	2929 sh	2933 sh	2938 sh	
$\nu_5(\text{C–H})$ stretch or $2\nu_4(\text{NH}_4^+)$	2870 m	2887 m	2894 m	
$2\nu_5$	2755 w	2742 w	2743 w	
$\delta_{\text{as}}(\text{N–H})$ , $\nu_2$	1690 sh	1691 sh	1689 sh	
$\nu_4(\text{OCO})$ stretch, asym	1575 s	1583 s	1583 s	
$\nu_4(\text{NH}_4^+)$	1441 m	1442 m	1445 m	
$\nu_5(\text{OCO})$ deformation, asym	1389 s	1379 sh		
$\nu_2(\text{OCO})$ stretch, sym	1367 s	1372 s	1372 s	
$\nu_6$ out-of-plane deformation	1074 vw	1070 vw	1072 vw, 1023 vw	
		949 br, vw		
$\nu_6$ OCO deformation, sym	795 s	807 s	815 s	

UV–Vis			
<b>1Mn</b>	<b>2Co</b>	<b>3Ni</b>	
17900 w, ${}^6\text{A}_{1\text{g}} \rightarrow {}^4\text{T}_{1\text{g}}(\text{G})$	16000 sh, ${}^4\text{T}_{1\text{g}}(\text{F}) \rightarrow {}^4\text{A}_{2\text{g}}(\text{F})$	13600 s, ${}^3\text{A}_{2\text{g}}(\text{F}) \rightarrow {}^1\text{E}_{\text{g}}(\text{D})$	
24600 w, ${}^6\text{A}_{1\text{g}} \rightarrow {}^4\text{T}_{2\text{g}}(\text{G})$	19300 s, ${}^4\text{T}_{1\text{g}}(\text{F}) \rightarrow {}^4\text{T}_{2\text{g}}(\text{F})$	14900 s, ${}^3\text{A}_{2\text{g}}(\text{F}) \rightarrow {}^3\text{T}_{1\text{g}}(\text{F})$	
27400 w, ${}^6\text{A}_{1\text{g}} \rightarrow {}^4\text{E}_{\text{g}}(\text{D})?$	21400 sh, ${}^4\text{T}_{1\text{g}}(\text{F}) \rightarrow {}^4\text{T}_{1\text{g}}(\text{P})$	21500 sh, ${}^3\text{A}_{2\text{g}}(\text{F}) \rightarrow ?$	
		25100 s, ${}^3\text{A}_{2\text{g}}(\text{F}) \rightarrow {}^3\text{T}_{1\text{g}}(\text{P})$	

<sup>a</sup> Key: s, strong; m, medium; w, weak; vw, very weak; sh, shoulder; br, broad.

**1Mn** and **2Co**, the first weight loss occurred at ca. 190 and 220 °C, respectively. It corresponds to the lost of one ammonia and one formic acid per formula resulting in the formation of the binary phase with the stoichiometry of  $\text{M}(\text{HCOO})_2$ . This phase is stable up to ca. 330 and 280 °C, respectively, where it decomposes into the corresponding metal oxide, MO. The two processes are endothermic under nitrogen. From the DSC, an estimation of the energy required for the two processes is similar, ca. 130 kJ mol<sup>−1</sup>. The experimental (calculated) percentage weight loss for the first process is 30.4 (30.3) and 28.9 (29.7) for **1Mn** and **2Co**, respectively. For the second step, the corresponding weight losses are within 2% of those calculated on the basis of residues of MnO and CoO. In contrast, **3Ni** shows one step of weight loss at ca. 240 °C. It is also endothermic, with an energy requirement of 220 kJ mol<sup>−1</sup>, roughly the sum of the

energy consumption for the two thermal processes for **1Mn** and **2Co**. This indicates that for **3Ni** the loss of ammonia and formic acid and the decomposition of  $\text{Ni}(\text{HCOO})_2$  are not separable. The final residue for **3Ni** (at 800 °C) is within 1.5% of that calculated on the basis of NiO. The results suggest that the stability of the ammonium salts decreases with increasing size of the ionic radii of the metal in the order  $\text{Mn} < \text{Co} \sim \text{Ni}$ . In comparison with previous results on other salts with larger amines,<sup>24</sup> we note slight changes in the temperature of the transformation into  $\text{M}(\text{HCOO})_2$ . However, the stability of  $\text{M}(\text{HCOO})_2$  has the reverse order. It should be pointed out that the three compounds in the present work have thermal stability similar to that of the perovskite compounds  $[\text{AmineH}][\text{M}(\text{HCOO})_3]$ <sup>24</sup> but lower than that of the more robust nanoporous diamond framework compounds of  $[\text{M}_3(\text{HCOO})_6]$ .<sup>18–21</sup>



**Table 4.** Summary of Magnetic Properties of **1Mn**, **2Co**, and **3Ni**

	<b>1Mn</b>	<b>2Co</b>	<b>3Ni</b>
$C^a/cm^3 K mol^{-1}$	4.64	3.92	1.29
$\Theta^b/K$	-11.2	-57.5	-61.1
$\chi T(300 K)/cm^3 K mol^{-1}$	4.37	3.21	1.08
$T_N^c/K$	8.4	9.8, 6.0	29.5
$T_p^d/K$	7.8	9.6, 5.8	29.0
$(J^e/k_B)/K$	-0.32	-3.8	-7.6
$H_c^f/Oe$ (at 2 K)		400	830
$M_s^g/cm^3 G mol^{-1}$ (at 2 K)		25	50
$H_{SF}^h/kOe$ (at 2 K)	0.6	14	>50

<sup>a</sup> Curie constants. <sup>b</sup> Weiss constants. <sup>c</sup> Critical temperatures based on ZFC/FC measurements. <sup>d</sup> Temperatures at peak positions in ac measurements at zero dc field. <sup>e</sup> Estimated by  $J/k_B = 3\Theta/[2zS(S+1)]$ . <sup>f</sup> Coercive field. <sup>g</sup> Remnant magnetization. <sup>h</sup> Peak positions in  $dM/dH$ .

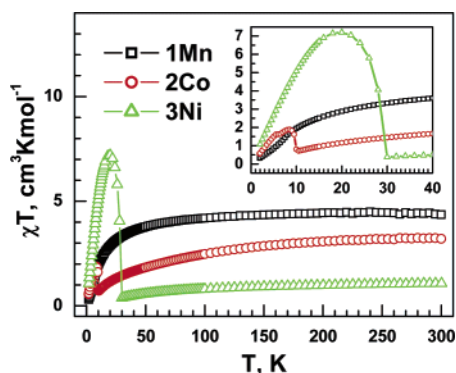


**Figure 2.** Plots of  $\chi T$  vs  $T$  for **1Mn**, **2Co**, and **3Ni** in an applied field of 100 Oe. The inset shows the low-temperature region.

**Magnetic Properties.** The investigation of the magnetic properties reveals that **1Mn**, **2Co**, and **3Ni** are antiferromagnets with the later two showing weak ferromagnetism at low temperatures. The basic magnetic parameters are listed in Table 4. Therefore, we will discuss the properties first in the paramagnetic region and then in the low-temperature region.

The temperature dependence of magnetic susceptibility, measured in an applied field of 100 Oe for **1Mn**, **2Co**, and **3Ni** (Figure 2), shows mainly antiferromagnetic character. At room temperature, the  $\chi T$  values, being 4.37, 3.21 and 1.08  $cm^3 K mol^{-1}$  for **1Mn**, **2Co**, and **3Ni**, respectively, are close to those expected for the  $M^{2+}$  ions.<sup>37</sup> On lowering of the temperature from 300 to 50 K, the  $\chi T$  values decrease slowly and then decrease more rapidly. The susceptibility data in the high-temperature region (above 20, 50, and 60 K for **1Mn**, **2Co**, and **3Ni**, respectively) can be fitted to the Curie–Weiss law with  $C = 4.64, 3.92$ , and  $1.29 cm^3 K mol^{-1}$  and  $\Theta = -11.2, -57.5$ , and  $-61.1 K$ , respectively. These negative Weiss temperatures correspond to antiferromagnetic exchange interactions between nearest neighbors. In the low-temperature region, different magnetic behaviors are observed (Figure 2, inset). **1Mn** shows a discontinuity around 7 K in  $\chi T$  followed by a faster decrease to  $0.31 cm^3 K mol^{-1}$  at 1.9 K. For **2Co**, the  $\chi T$  value goes to a minimum of  $0.72 cm^3 K mol^{-1}$  around 10 K and then rises sharply to a maximum of  $1.88 cm^3 K mol^{-1}$  at 8.5 K. After the maximum, a second

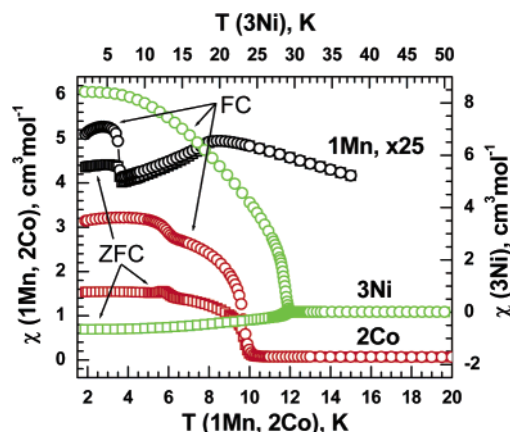


**Figure 3.** ZFC/FC measurements under 5 Oe field for **1Mn**, **2Co**, and **3Ni**. The negative ZFC values of **3Ni** were due to the small negative residual field of the zero field setting of the SQUID instrument and easy magnetization of the sample.

turn in  $\chi T$  around 6 K is observed, followed by a decrease of  $\chi T$  to  $0.56 cm^3 K mol^{-1}$  at 1.9 K. After a minimum of  $0.41 cm^3 K mol^{-1}$  at 30 K, the  $\chi T$  value of **3Ni** displays a sharp rise to a broad maximum of  $7.20 cm^3 K mol^{-1}$  at ca. 20 K, and then it decreases again to  $1.07 cm^3 K mol^{-1}$  at 2 K. From these data it appears that in the low-temperature region **1Mn** is a simple antiferromagnet while **2Co** and **3Ni** are weak ferromagnets, and for **2Co** the two magnetic phase transitions are observed around 9 and 6 K.

The magnetism in the low-temperature region for these compounds was further investigated by measuring the magnetization in the low field following zero-field (ZFC) and field-cooled (FC) protocol (Figure 3) and the ac susceptibility (Figure S6). **1Mn** displays a broad maximum in both ZFC/FC with the in-phase  $\chi'$  around 8 K confirming the antiferromagnetic ground state (Figures 3 and S6a). At 3.6 K, a sudden increase of the dc susceptibility was observed, and at the same temperature, peaks of both  $\chi'$  and  $\chi''$ , though very weak in  $\chi'$  (star marked in Figure S6a), were observed. It is possible that the 3.6 K transition might result from a very small amount of  $Mn(HCOO)_2 \cdot 2H_2O$  impurity in the samples given that its transition temperature is very close to 3.7 K.<sup>12c–h</sup> For **2Co**, the ZFC/FC magnetizations show clearly two transitions at 9.8 and 6.0 K (Figure 3). The lower temperature transition is higher than observed for  $Co(HCOO)_2 \cdot 2H_2O$  at 5.1 K,<sup>12i,m</sup> confirming the absence of the dihydrate salt. Meanwhile in ac susceptibility data (Figure S6b) both  $\chi'$  and  $\chi''$  display two sharp peaks at 9.6 and 5.8 K that are compatible with ZFC/FC dc susceptibility. The strength of the lower temperature peak is more significant than that at higher temperature. In addition to the phase purity proved by PXRD (Figure S1), the ZFC/FC measurement (Figure S7) for five carefully selected, randomly oriented, clean crystals gave the same results as described before on a polycrystalline sample of 10 mg (Figure 3). Similarly, two magnetic transitions was reported for the perovskite compounds of  $[(CH_3)_2NH_2][Co(HCOO)_3]$ ,<sup>24a</sup> where the two transition temperatures are 14.9 and 13.1 K. These might arise from a spin-reorientation and will need further investigation. For **3Ni**, the transition at 29.5 K from the ZFC/FC

(37) Casey, A. T.; Mitra, S. In *Theory and Application of Molecular Paramagnetism*; Mulay, L. N., Boudreaux, E. A., Eds.; John Wiley & Sons Inc.: New York, 1976; p 184.

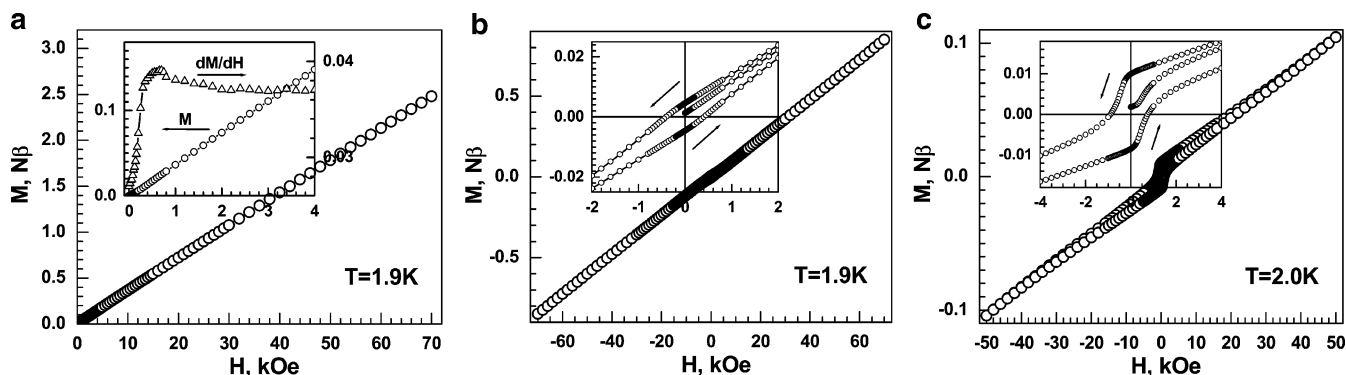


**Figure 4.** Isothermal magnetizations for (a) **1Mn**, (b) **2Co**, and (c) **3Ni**. The inset shows the low-field region.

measurements (Figure 3) and peak around 29.5 K in ac data for both  $\chi'$  and  $\chi''$  (Figure S6c) confirm the magnetic transition. Finally, the weak ferromagnetism of **2Co** and **3Ni** is confirmed by the spontaneous magnetizations observed in ZFC/FC under low fields.

The critical temperatures ( $T_N$ 's) of **1Mn**, **2Co** (the first  $T_N$ ), and **3Ni** (Table 4) are close to and in the same sequence as the recently reported perovskite formate compounds of  $[\text{AmineH}^+][\text{M}(\text{HCOO})_3]$  of the  $\text{M} = \text{Mn}$  (7.6–8.5 K),  $\text{Co}$  (14.9 K for  $[(\text{CH}_3)_2\text{NH}_2][\text{Co}(\text{HCOO})_3]$ ), and  $\text{Ni}$  (35.6 K for  $[(\text{CH}_3)_2\text{NH}_2][\text{Ni}(\text{HCOO})_3]$ ) series,<sup>24</sup> with the same numbers of *anti-anti* HCOO links between metal ions and similar local coordination environment around metal ions, though the framework topologies are different. It is worth noting that the  $\text{Ni}$  compound **3Ni** has a considerably high critical temperature of ca. 30 K; this might be of interest for the chiral magnet. These critical temperatures are in the same sequence and two times higher than those of the related metal formate dihydrates  $\text{M}(\text{HCOO})_2 \cdot 2\text{H}_2\text{O}$  which are all 2D antiferromagnets with  $T_N$ 's of 3.7, 5.1, and 15.5 K for  $\text{M} = \text{Mn}$ ,  $\text{Co}$ , and  $\text{Ni}$ , respectively.<sup>12</sup> It is as expected that the higher critical temperatures of the perovskite compounds of  $[\text{AmineH}^+][\text{M}(\text{HCOO})_3]$  and the compounds of this work are due to the higher dimensionality (3D) of the frameworks compared to the 2D ones of  $\text{M}(\text{HCOO})_2 \cdot 2\text{H}_2\text{O}$ , given the very similar metal–metal linkages and thus similar magnitudes of exchange coupling.

In the isothermal magnetization measurement at 2 K (Figure 4), **1Mn** shows no noticeable hysteresis, but a small kink in the magnetization versus field is observed at ca. 600 Oe (Figure 4a). At higher field the magnetization increases linearly and reaches ca.  $2.5 N\beta$  at the highest applied field of 70 kOe being half of the saturation value of  $5 N\beta$  for  $\text{Mn}^{2+}$  ( $S = 5/2$  and  $g = 2.00$ ). This indicates a spin-flop transition for the compound at 600 Oe. The magnetism of **1Mn** is similar to that of the perovskite compounds,  $[\text{AmineH}^+][\text{Mn}(\text{HCOO})_3]$ .<sup>24b</sup> However, there is no indication of weak ferromagnetism at the Néel transition as in the perovskite Mn compounds. For **2Co** and **3Ni** (Figure 4b,c), hysteresis is observed in the isothermal magnetization (Figure 4b,c, inset), with the remnant magnetization and coercive field being  $25 \text{ cm}^3 \text{ G mol}^{-1}$  and 400 Oe for **2Co**, and  $50 \text{ cm}^3 \text{ G mol}^{-1}$  and 830 Oe for **3Ni**, respectively. Spontaneous magnetization in very low applied field together with the low magnetization values of tens of  $\text{cm}^3 \text{ G mol}^{-1}$  and the

linear dependence at high field characterize the weak ferromagnetism or spin-canting in the two materials. Weak ferromagnetism has also been observed for the related perovskite compounds of  $[\text{AmineH}^+][\text{M}(\text{HCOO})_3]$  with  $\text{M} = \text{Co}$  and  $\text{Ni}$ .<sup>24a</sup> The spin-flop transitions in **2Co** and **3Ni** occur at much higher fields than that for **1Mn**, being 14 kOe (**2Co**) and possibly above 50 kOe (**3Ni**), while the magnetizations at the highest applied field, 0.85 and  $0.11 N\beta$  for **2Co** and **3Ni**, respectively, are also far from the expected saturation values for  $\text{Co}^{2+}$  and  $\text{Ni}^{2+}$ . From the remnant magnetizations the canting angle is estimated<sup>38</sup> to be  $0.1^\circ$  for **2Co** and  $0.2^\circ$  for **3Ni**, respectively.

For this particular framework topology no suitable model is available for estimating the coupling constant  $J$  between nearest  $\text{M}^{2+}$  neighbors bridged by *anti-anti* formate ligand. Therefore, the molecular field result  $J/k_B = 3\Theta/[2zS(S+1)]$  was used.<sup>39</sup> With  $z = 6$ ,  $S = 5/2$ ,  $3/2$ , and 1 for **1Mn**, **2Co**, and **3Ni**, respectively, and the Weiss temperatures,  $\Theta$ 's, we estimate the  $J/k_B$  values of  $-0.32$ ,  $-3.8$  and  $-7.6$  K for **1Mn**, **2Co**, and **3Ni**, respectively. These estimations are close to  $-0.35$ ,  $-4.3$ , and  $-8.6$  K of  $\text{M}(\text{HCOO})_2 \cdot 2\text{H}_2\text{O}$ <sup>12</sup> and  $\text{M}(\text{HCOO})_2 \cdot 2\text{L}$ ,<sup>13</sup> as well as those of the recently reported  $[\text{AmineH}^+][\text{M}(\text{HCOO})_3]$ ,<sup>24</sup> with  $\text{M} = \text{Mn}$  ( $-0.34$  to  $-0.37$  K),  $\text{Co}$  ( $-3.4$  K), and  $\text{Ni}$  ( $-7.3$  K), both possessing similar *anti-anti* HCOO linkages.

It is well-known that spin canting may be a result of antisymmetric exchange and/or single-ion anisotropy.<sup>33</sup> As mentioned before, the structures satisfy the requirement for the Dzyaloshinsky–Moriya interaction, i.e., the antisymmetric exchange between magnetic metal sites, as found for other metal formates.<sup>12,13,14,24</sup> For **2Co** and **3Ni**, the single-ion anisotropy of  $\text{Co}^{2+}$  and  $\text{Ni}^{2+}$  enhances the Dzyaloshinsky–Moriya interaction because the antisymmetric exchange is proportional to the single-ion anisotropy. Neutron diffraction experiments, as well as very low-temperature structure determinations, are needed for understanding the detailed magnetic structures.

## Conclusion

In summary, employing the smallest and simplest ammonium results in the series of chiral magnets  $[\text{NH}_4]$ -

(38) Kahn, O. *Molecular Magnetism*; John Wiley & Sons Inc.: New York, 1993; p 322.

(39) Carlin, R. L. *Magnetochemistry*; Springer-Verlag: Berlin, Heidelberg, Germany, 1986; p 149.



[M(HCOO)<sub>3</sub>] (M = Mn, Co, and Ni). The structure possesses a rarely observed 4<sup>9</sup>·6<sup>6</sup> topology and channels occupied by linear NH<sub>4</sub><sup>+</sup> arrays. This result, together with the previous reports, demonstrates clearly the template effect of the protonated amine cations for the formation of different metal–formate frameworks. It also revealed that chirality can be produced from such simple achiral starting components. The Mn compound is an antiferromagnet ( $T_N = 8.4$  K and low spin-flop field of 600 Oe), while both Co and Ni compounds exhibit weak ferromagnetism ( $T_N = 9.8$  K (Co) and 29.5 K (Ni)) and there is a second transition at 5.8 K for **2Co** probably due to spin-reorientation. The estimated couplings,  $J/k_B$ , using the molecular field approximation are  $-0.32$  (Mn),  $-3.8$  (Co), and  $-7.6$  K (Ni). The weak ferromagnetism arises from the antisymmetric exchange via the noncentrosymmetric HCOO bridges, enhanced by single-ion anisotropy for the Co and Ni compounds. The compounds are fairly stable up to ca. 200 °C. The strong absorption bands of the chiral magnetic salts of Co and Ni in the visible region

render them attractive for possible magneto–optical properties, and this merit further study when homochiral samples are available. Finally, that many formate compounds are magnets with interesting and abundant magnetism gives us more inspiration to use the simple formate ligands in future studies.

**Acknowledgment.** This work is supported by the CREST, Japan Science and Technology Corp., Chinese Academy of Sciences, CMS-CX200510, and NSFC (Grants 20571005, 20473095, 20490210, and 20221101). We thank Prof. Stuart R. Batten of the School of Chemistry of Monash University, Monash, Australia, for his kind help in discussion of the network topology.

**Supporting Information Available:** Figure S1–S7 and CIF files of crystallography data for the structures in this work. This material is available free of charge via the Internet at <http://pubs.acs.org>.

IC0610031